[16] P. Schniter and S. Rangan, "Compressive phase retrieval via generalized approximate message passing," *IEEE Trans. Signal Process.*, vol. 64, no. 4, pp. 1043–1055, Feb. 2015.

[17] P. Maechler *et al.*, "VLSI design of approximate message passing for signal restoration and compressive sensing," *IEEE Trans. Emerging Sel. Topics Circuits Syst.*, vol. 2, no. 3, pp. 579–590, Sep. 2012.

Nonorthogonal Time–Frequency Training-Sequence-Based CSI Acquisition for MIMO Systems

Wenbo Ding, *Student Member, IEEE*, Fang Yang, *Senior Member, IEEE*, Sicong Liu, *Student Member, IEEE*, Xianbin Wang, *Senior Member, IEEE*, and Jian Song, *Senior Member, IEEE*

***Abstract*—In this paper, a spectrally efficient nonorthogonal time–frequency training sequence (TS)-based channel state information (CSI) acquisition approach is proposed for multiple-input–multiple-output orthogonal frequency-division multiplexing (MIMO-OFDM) systems under the framework of structured compressed sensing (SCS). The scheme first relies on a time-domain TS that is identical for all transmit antennas to acquire the partial channel common support by utilizing the spatial correlation property of the MIMO channels and then uses the frequency-domain TS for accurate CSI recovery based on the proposed adaptive spatially–temporally joint simultaneous orthogonal matching pursuit algorithm. Here, the obtained partial channel common support can be utilized to reduce the complexity of the classical SCS algorithm and improve the signal recovery probability. Simulation results show that the proposed scheme could significantly reduce the TS overhead and demonstrate better performance than the existing MIMO-OFDM systems, which might be suitable for massive MIMO systems in future fifth-generation communications.**

***Index Terms*—Channel state information (CSI) acquisition, multiple-input multiple-output (MIMO), nonorthogonal time–frequency training sequence (TS), spatial–temporal correlations, structured compressed sensing (SCS).**

I. Introduction

Multiple-input multiple-output (MIMO) has attracted much interest from both academia and industry due to its outstanding capability to significantly increase system capacity and spectral efficiency [1]. Consequently, the MIMO technique has been widely employed by the most advanced wireless communication systems, such as Long-Term Evolution [1], IEEE 802.11ad [2], etc., and, at the same time, is considered as a promising technique for future fifth-generation (5G) wireless communications [3].

In practical MIMO systems, accurate knowledge of the channel state information (CSI) is a prerequisite at the transmitter and/or the receiver to exploit the advantages that MIMO can offer, including beamforming, precoding, and so on [4]. Hence, there has been plenty of work on CSI acquisition for MIMO systems, among which, the training sequence (TS)-based approaches, relying on the known TS to acquire the CSI, are more reliable and commonly adopted [5], [6].

According to the multiplexing way between the TS and the data, the TS-based approaches can be categorized into two types, namely, the time-domain [5] and frequency-domain [6] TS-based approaches. However, the conventional TS-based approaches have one main drawback, which is that the TSs of different antennas have to be orthogonal in either the time or the frequency domain and, hence, are not spectrally efficient when the scale of the antenna number is very large, i.e., in massive MIMO scenarios [7], or the channels are undergoing severe time varying, where CSI acquisition has to be performed very frequently, for example, every frame [8]. Recently, by exploiting the channel sparsity of the MIMO systems, the compressive sensing (CS) theory is applied to reduce the orthogonal TS overhead for each antenna [9]. Furthermore, some researchers consider the channel correlations and use the nonorthogonal frequency-domain TS occupying the same subcarriers to acquire the CSI based on the structured CS (SCS) [10]–[12].

In this paper, to further improve the spectral efficiency and system performance, we propose a nonorthogonal time–frequency TS-based CSI acquisition approach for MIMO systems under the framework of SCS [10]. Specifically, the contributions of this paper can be summarized as follows.

1) In contrast to the existing schemes where the nonorthogonal TS lies solely in the frequency domain [11], [12], there exist both nonorthogonal time- and frequency-domain TSs in the proposed scheme. Therefore, the time-domain TS, which is identical for all transmit antennas and transmitted in the same time slot, can work as the guard interval and be used to obtain the partial channel common support, whereas the different frequency-domain TSs occupying the same subcarriers for different transmit antennas are used for accurate CSI acquisition.
2) By utilizing the obtained partial channel common support and the channel spatial–temporal correlations, an adaptive spatially–temporally joint simultaneous orthogonal matching pursuit (AST-SOMP) algorithm is proposed for accurate CSI recovery. Compared with the standard SOMP algorithm, the proposed algorithm reduces the required number of observations for reliable recovery and has lower complexity and better performance.
3) Compared with the schemes with structured subspace pursuit (SSP) or block orthogonal matching pursuit (BOMP) [11], [12] and the conventional schemes [5], [6], the proposed scheme demonstrates higher spectral efficiency and lower complexity by modifying the well-known low-complexity SOMP algorithm.

The remainder of this paper is organized as follows. The system model, including the TS pattern design, is introduced in Section II. The proposed CSI acquisition method based on the AST-SOMP algorithm is addressed in Section III. Sections IV and V provide the performance analysis and the simulation results, respectively. Finally, conclusions are drawn in Section VI.

Manuscript received December 5, 2014; revised June 17, 2015; accepted July 29, 2015. Date of publication August 3, 2015; date of current version July 14, 2016. This work was supported in part by the National Natural Science Foundation of China under Grant 61401248 and Grant 61471219, by the New Generation Broadband Wireless Mobile Communication Network of the National Science and Technology Major Projects under Grant 2015ZX03002008, by the Tsinghua University Initiative Scientific Research Program under Grant 2014Z06098, and by the Science and Technology Project of State Grid Corporation of China under Grant SGHAZZ00FCJS1500238. The review of this paper was coordinated by Dr. A. J. Al-Dweik.

W. Ding, F. Yang, S. Liu, and J. Song are with the Department of Electronic Engineering, Tsinghua University, Beijing 100084, China, and also with the Research Institute of Information Technology, Tsinghua National Laboratory for Information Science and Technology (TNList), Tsinghua University, Beijing 100084, China (e-mail: dwb11@mails.tsinghua.edu.cn; liu-sc12@mails.tsinghua.edu.cn; fangyang@tsinghua.edu.cn; jsong@tsinghua.edu.cn).

X. Wang is with the Department of Electrical and Computer Engineering, University of Western Ontario, London, ON N6A 5B9, Canada (e-mail: xianbin.wang@uwo.ca).

Color versions of one or more of the figures in this paper are available online at http://ieeexplore.ieee.org.

Digital Object Identifier 10.1109/TVT.2015.2463716

Notation: We use the lowercase and uppercase boldface letters to denote vectors and matrices. $(\cdot)^T$, $(\cdot)^H$, $(\cdot)^{-1}$, $\mathbf{diag}(\cdot)$, and $\|\cdot\|_p$ denote the transpose, conjugate transpose, matrix inversion, diagonal matrix, and l_p-norm operations, respectively; $\mathbf{x}_\Omega$ denotes the entries of vector $\mathbf{x}$ in the set of Ω; and $\mathbf{\Phi}_\Pi$ represents the submatrix comprising the Π columns of $\mathbf{\Phi}$.

II. System Model

A. Spatial–Temporal Correlations of Sparse MIMO Channels

For an $N_t \times N_r$ MIMO system consisting of N_t transmit and N_r receive antennas, the L-length channel impulse response (CIR) associated with the pth $(1 \le p \le N_t)$ transmit antenna and a certain receive antenna[1] during the ith frame can be modeled as [5], [6]

$$\mathbf{h}_i^{(p)} = \left[h_{i,0}^{(p)}, h_{i,1}^{(p)}, \ldots, h_{i,L-1}^{(p)}\right]^T. \tag{1}$$

Due to the physical properties of outdoor electromagnetic propagation, the CIRs in wireless communications are usually modeled to be sparse [13], [14]. The support, i.e., the nonzero index of $\mathbf{h}_i^{(p)}$ can be written as $T_i^{(p)} = \{l : |h_{i,l}^{(p)}| > 0\}_{l=0}^{L-1}$.

Moreover, the support is identical for all the channels associated with different transmit antennas, which is referred to as the spatial correlation [14], [15]. This property follows from the fact that the propagation delay is roughly the same for all transmit–receive antenna pairs.

On the other hand, it has been observed that the path delays of the practical wireless channels usually vary much slower than the path gains [14], i.e., even if the path gains are varying significantly from one frame to the next, the path delays among several successive frames still remain unchanged, which is referred to as the temporal correlation. The temporal correlation can be assumed during R adjacent frames, where R is associated with the channel coherence time.

In this paper, we will fully exploit the spatial–temporal correlations of sparse MIMO channels and design a more spectrally efficient CSI acquisition approach with the nonorthogonal time–frequency TSs.

B. MIMO-OFDM With Nonorthogonal Time–Frequency TSs

Fig. 1 presents the frame structures of different TS-based MIMO orthogonal frequency-division multiplexing (OFDM) schemes. As shown in Fig. 1(a), the orthogonal time-domain TS-based scheme uses the TSs multiplexed in the time domain to obtain the CSI for each transmit antenna [5]. To ensure the estimation accuracy, the length of each TS M should be no less than the channel length, i.e., $M \ge L$. Hence, the total TS overhead will be larger than $N_t L$. In Fig. 1(b), the orthogonal frequency-domain TS-based scheme utilizes the comb-type orthogonal TSs for CSI acquisition, whereby the effective TSs are nonoverlapping, and nulls (zeros) are also inserted to prevent the mutual TS contamination among different transmit antennas [6]. Here, the cyclic prefix (CP) is placed before the OFDM block as the guard interval to avoid the interblock interference (IBI). However, in the orthogonal TS-based schemes, the TS overhead will dramatically increase as the number of antennas goes up.

To improve the spectral efficiency, the scheme adopting the nonorthogonal frequency-domain TS for CSI acquisition is proposed by exploiting the channel sparsity and correlations [11], [12]. As shown in Fig. 1(c), the "nonorthogonal" here means that the TSs of different transmit antennas occupy the same subcarriers in the frequency domain. By exploiting the channel sparsity and correlation, researchers propose the SSP and BOMP algorithms [11], [12] to significantly reduce the TS overhead.

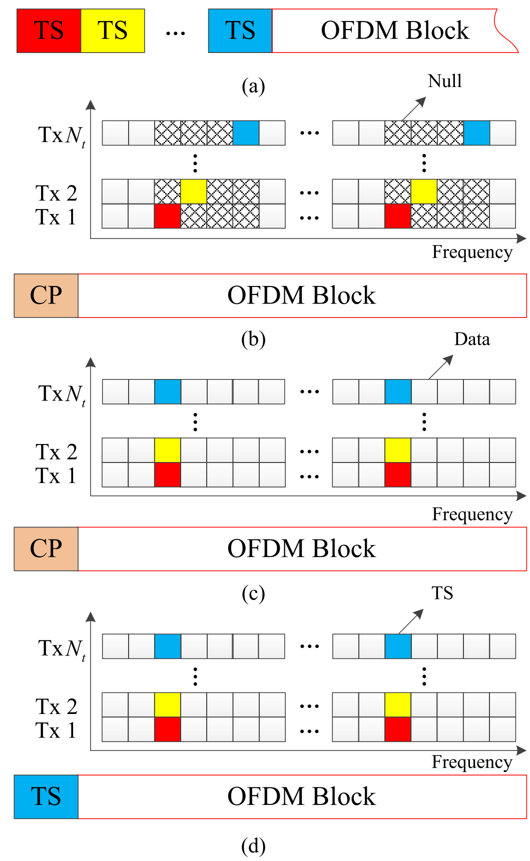

Fig. 1. Frame structures of different MIMO-OFDM schemes. (a) Orthogonal time-domain TS-based MIMO-OFDM scheme. (b) Orthogonal frequency-domain TS-based MIMO-OFDM scheme. (c) Nonorthogonal frequency-domain TS-based MIMO-OFDM scheme. (d) Proposed nonorthogonal time–frequency TS-based MIMO-OFDM scheme.

Unlike conventional schemes, the proposed MIMO-OFDM has both nonorthogonal time- and frequency-domain TSs for every frame, as shown in Fig. 1(d). The ith frame of the pth transmit antenna consists of an M-length TS $\mathbf{c} = [c_0, c_1, \ldots, c_{M-1}]^T$ and an N-length OFDM block $\mathbf{x}_i^{(p)} = [x_{i,0}^{(p)}, x_{i,1}^{(p)}, \ldots, x_{i,N-1}^{(p)}]^T = \mathbf{F}^H \tilde{\mathbf{x}}_i^{(p)}$, where $\mathbf{F}$ is the $N \times N$ discrete Fourier transform (DFT) matrix. The nonorthogonal time-domain TS is an identical sequence and will be simultaneously transmitted for all transmit antennas, which should have a good autocorrelation property for both synchronization and partial channel common support acquisition. $\tilde{\mathbf{x}}_i^{(p)}$ denotes the frequency-domain OFDM block that contains a small amount N_P of the TS on the location of $\mathcal{D} = \{d_n\}_{n=0}^{N_P-1}$.

At the receiver, after removing the interference from the TS and the cyclicity reconstruction for OFDM blocks, the received frequency-domain OFDM block can be written as

$$\tilde{\mathbf{y}}_i = \sum_{p=1}^{N_t} \mathbf{diag}\left(\tilde{\mathbf{x}}_i^{(p)}\right) \mathbf{F}_L \mathbf{h}_i^{(p)} + \mathbf{w}_i \tag{2}$$

where $\mathbf{F}_L$ is the $N \times L$ partial DFT matrix containing the first L columns of $\mathbf{F}$. Since we only focus on the received pilots located at $\mathcal{D}$,

[1] As the processing is identical for every receive antenna, the receive antenna index will be omitted for simplification.

(2) can be simplified as

$$\tilde{\mathbf{y}}_{i,\mathcal{D}} = \sum_{p=1}^{N_t} \mathbf{diag}\left(\tilde{\mathbf{x}}_{i,\mathcal{D}}^{(p)}\right) \mathbf{F}_{\mathcal{D}} \mathbf{h}_i^{(p)} + \mathbf{w}_{i,\mathcal{D}} \quad (3)$$

where $\mathbf{F}_{\mathcal{D}}$ is the $N_P \times L$ partial DFT matrix with the $(n+1, k+1)$th entry being $\exp(-j2\pi d_n k/N)/\sqrt{N}$. By defining $\mathbf{D}^{(p)} \triangleq \mathbf{diag}(\tilde{\mathbf{x}}_{i,\mathcal{D}}^{(p)})$, (3) can be rewritten in a matrix form as

$$\begin{aligned}\tilde{\mathbf{y}}_{i,\mathcal{D}} &= \left[\mathbf{D}^{(1)}\mathbf{F}_{\mathcal{D}}, \mathbf{D}^{(2)}\mathbf{F}_{\mathcal{D}}, \ldots, \mathbf{D}^{(N_t)}\mathbf{F}_{\mathcal{D}}\right]_{N_P \times N_t L} \mathbf{h}_i + \mathbf{w}_{i,\mathcal{D}} \\ &\triangleq \mathbf{\Phi}\mathbf{h}_i + \mathbf{w}_{i,\mathcal{D}} \quad (4)\end{aligned}$$

where $\mathbf{h}_i = [(\mathbf{h}_i^{(1)})^T, (\mathbf{h}_i^{(2)})^T, \ldots, (\mathbf{h}_i^{(N_t)})^T]^T$ is the equivalent CIR vector of size $N_t L \times 1$. Afterward, by utilizing the channel sparsity, $\mathbf{h}_i$ can be reconstructed by the structured CS method, which will be detailed in Section III.

C. TS Pattern Design

The TS pattern design in this paper includes the nonorthogonal TSs in both the time and frequency domains.

To obtain the partial channel common support, the time-domain TSs for different transmit antennas should be identical and have a good autocorrelation property. Considering the peak-to-average power ratio requirements of the practical systems, the constant-amplitude zero-autocorrelation sequences would be a feasible choice [16].

On the other hand, according to the CS theory, the recovery performance is guaranteed by the restricted isometry property (RIP) of the observation matrix $\mathbf{\Phi}$ [17]. From the structure of $\mathbf{\Phi}$ in (4), we could find that the RIP of $\mathbf{\Phi}$ is determined by the choice of $\{\mathbf{D}^{(p)}\}_{p=1}^{N_t}$ and $\mathbf{F}_{\mathcal{D}}$, or equivalently, the TS $\{\tilde{\mathbf{x}}_{i,\mathcal{D}}^{(p)}\}_{p=1}^{N_t}$ and the location $\mathcal{D}$. Since better randomness of $\{\tilde{\mathbf{x}}_{i,\mathcal{D}}^{(p)}\}_{p=1}^{N_t}$ and $\mathcal{D}$ leads to the better RIP of $\mathbf{\Phi}$, one possible way to design the frequency-domain TSs can be realized by generating N_t sequences of each length N_P according to the independently and identically distributed random Bernoulli distribution (± 1) [11].

III. Time–Frequency Joint Channel State Information Acquisition for Sparse Multiple-Input–Multiple-Output Systems

Here, by fully exploiting the time–frequency training feature of the proposed scheme and the spatial–temporal correlations of the sparse MIMO channels, we proposed the time–frequency joint CSI acquisition method based on the AST-SOMP algorithm. The proposed method is composed of three steps as follows.

A. Step 1: Time-Domain TS-Based Partial Channel Common Support Acquisition

Different from the conventional time-domain TS-based MIMO-OFDM systems where the TSs are used for accurate estimation [5], the proposed scheme utilizes the time-domain TS merely to acquire the partial channel common support. The length of the time-domain TS only needs to be no less than the channel length, i.e., $M \geq L$, and hence, the TS here can work as a guard interval as well.

At the receiver, we directly use the received TS $\hat{\mathbf{c}}_i$ without interference removal to correlate with the local TS, i.e.,

$$\bar{\mathbf{z}}_i = \frac{1}{MN_t}\mathbf{c} \otimes \hat{\mathbf{c}}_i = \frac{1}{N_t}\sum_{p=1}^{N_t} \mathbf{h}_i^{(p)} + \mathbf{v}_i \quad (5)$$

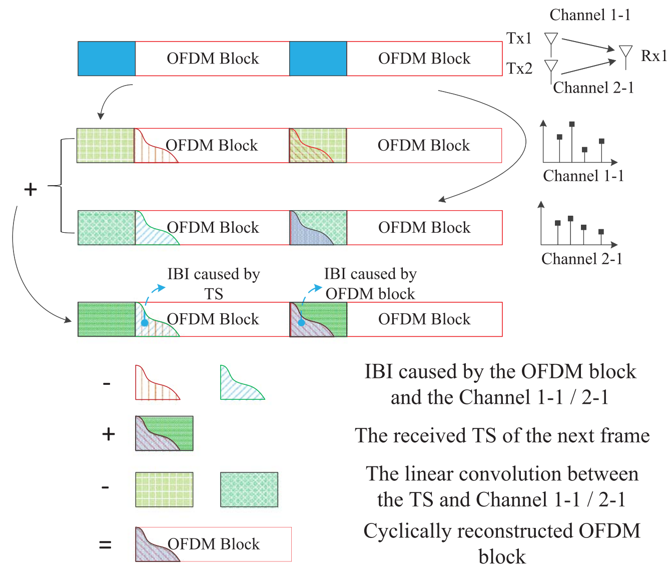

Fig. 2. OFDM block cyclicity reconstruction with two transmit antennas.

where $\otimes$ is the circular convolution operation, $\mathbf{v}_i$ denotes the interference including the channel noise and the IBI, and the correlation result $\bar{\mathbf{z}}_i$ is the rough estimate of the superposition of all the CIRs associated with the N_t transmit antennas.

By exploiting the spatial–temporal correlations of the channel, the partial channel common support $T_0 = \{l: \sum_{j=i}^{i+R-1} \|\bar{z}_{j,l}\|_2 / R \geq a\}_{l=0}^{L-1}$ within the R frames can be obtained by appropriately selecting the threshold $a = 3(\sum_{j=i}^{i+R-1} \sum_{l=0}^{L-1} \|\bar{z}_{j,l}\|_2)^{1/2}/RL$ according to [18]. Meanwhile, the channel sparsity level, which is essential to the CS algorithm, can also be estimated by adding a positive compensation integer, i.e., $K = \|T_0\|_0 + b$ [13].

The obtained partial channel common support can be used to reduce the complexity and increase the reliability of the standard SCS algorithm, which will be detailed in ***Step 3***.

B. Step 2: Frequency-Domain TS Extraction Via OFDM Cyclicity Reconstruction

In the proposed nonorthogonal time–frequency TS-based MIMO-OFDM scheme, the standard CP [6] is replaced by the time-domain TS for channel information acquisition while sacrificing the cyclicity property of the received OFDM block over multipath fading channels. Hence, the cyclicity reconstruction is required to obtain the frequency-domain TS for accurate channel recovery.

The cyclicity reconstruction in this scheme can be achieved via the overlap-and-add operation [19], which could be summarized as follows.

1) For each transmit antenna, compute the IBI to the OFDM block caused by the time-domain TS and the CIR and then subtract them from the received OFDM block.
2) Add the received time-domain TS in the next frame to the received OFDM block. Here, the received time-domain TS contains the convolutional tails between the OFDM block of the current frame and the CIRs, as shown in Fig. 2.
3) For each transmit antenna, compute the linear convolution between the time-domain TS and the CIR and then subtract the first M symbols of the convolutional results from the received

OFDM block to obtain the cyclically reconstructed OFDM block.

The reconstruction process for two transmit antennas is provided for brief illustration, as shown in Fig. 2. After that, the frequency-domain TS can be extracted for accurate CIR estimation in ***Step 3***.

C. Step 3: Frequency-Domain TS-Based Accurate CIR Acquisition

Considering (4) during R adjacent frames and stacking the noisy measurements $\tilde{\mathbf{y}}_{i,\mathcal{D}}$ into one matrix $\mathbf{Y} = [\tilde{\mathbf{y}}_{i,\mathcal{D}}, \tilde{\mathbf{y}}_{i+1,\mathcal{D}}, \ldots, \tilde{\mathbf{y}}_{i+R-1,\mathcal{D}}]$, we have

$$\mathbf{Y} = \mathbf{\Phi}\mathbf{H} + \mathbf{W} \tag{6}$$

where $\mathbf{H} = [\mathbf{h}_i, \mathbf{h}_{i+1}, \ldots, \mathbf{h}_{i+R-1}]$ contains all the CIR information that needs to be estimated, and $\mathbf{W} = [\mathbf{w}_{i,\mathcal{D}}, \mathbf{w}_{i+1,\mathcal{D}}, \ldots, \mathbf{w}_{i+R-1,\mathcal{D}}]$. Due to the spatial–temporal correlations, the columns of $\mathbf{H}$ not only share the common sparse support but also have the inherent common structure, i.e., the support of $\mathbf{h}_i$ has a periodicity of L. Therefore, the problem formulated in (6) can be solved, and the recovery performance can be improved by the SCS algorithms [10].

Among the several SCS algorithms, the SOMP is well known and most frequently used due to its low complexity and relatively good performance [10] compared with the other high-performance but high-complexity algorithms [11], [12], which is more suitable for hardware implementation.

Based on the classical SOMP algorithm, we propose the AST-SOMP algorithm, which utilizes the partial channel common support obtained in ***Step 1*** and the inherent correlation in $\mathbf{h}_i$ to further reduce the complexity as well as improve the recovery performance. The proposed AST-SOMP algorithm is described in **Algorithm 1**.

Algorithm 1 Adaptive Spatially–Temporally Joint SOMP.

Inputs:
1) Initial channel common support T_0
2) Channel sparsity level K;
3) Noisy measurements $\mathbf{Y}$;
4) Observation matrix $\mathbf{\Phi}$.

Output: The K-sparse estimate $\mathbf{H} \triangleq \bar{\mathbf{H}}$.

Initial Configuration:

1: $\Pi \leftarrow T_0 \cup \{T_0 + L\} \cup \cdots \cup \{T_0 + (N_t - 1)L\}$; {Support Expansion due to Inherent Correlation.}

2: $\bar{\mathbf{H}}^{(0)} \leftarrow \mathbf{0}$; $\bar{\mathbf{H}}_{\Pi}^{(0)} \leftarrow (\mathbf{\Phi}_{\Pi}^H \mathbf{\Phi}_{\Pi})^{-1} \mathbf{\Phi}_{\Pi}^H \mathbf{Y}$; {Initial Signal Estimation.}

3: $\mathbf{R} \leftarrow \mathbf{Y} - \mathbf{\Phi}\bar{\mathbf{H}}^{(0)}$; {Initial Residual.}

Iterations:

4: **for** $k = 1 : K - \|T_0\|_0$ **do**

5: $\mathbf{P} \leftarrow \mathbf{\Phi}^H \mathbf{R}$; {Target Proxy Generation.}

6: $t \leftarrow \arg\max_i \sum_{j=0}^{R-1} \sum_{n=1}^{N_t} \|p_{i+(n-1)L,j}\|_1$; {Significant Entry Identification.}

7: $\Omega \leftarrow t \cup \{t + L\} \cup \cdots \cup \{t + (N_t - 1)L\}$; {Support Expansion due to Inherent Correlation.}

8: $\Pi \leftarrow \Pi \cup \Omega$; {Support Union.}

9: $\bar{\mathbf{H}}^{(k)} \leftarrow \mathbf{0}$; $\bar{\mathbf{H}}_{\Pi}^{(k)} \leftarrow (\mathbf{\Phi}_{\Pi}^H \mathbf{\Phi}_{\Pi})^{-1} \mathbf{\Phi}_{\Pi}^H \mathbf{Y}$; {Signal Estimation.}

10: $\mathbf{R} \leftarrow \mathbf{Y} - \mathbf{\Phi}\bar{\mathbf{H}}^{(k)}$; {Update Residual.}

11: **end for**

12: $\bar{\mathbf{H}} \leftarrow \bar{\mathbf{H}}^{(k)}$.

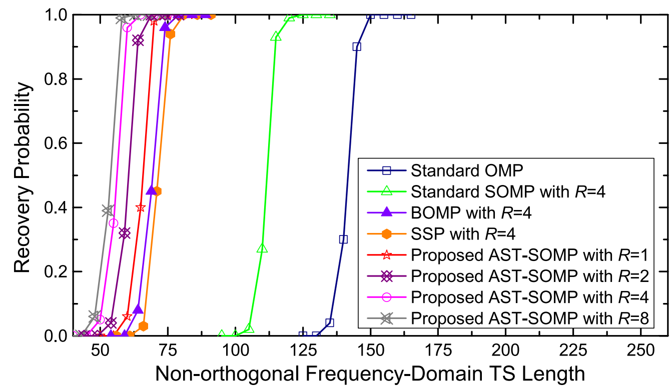

Fig. 3. Comparison of the CIR recovery probabilities at SNR = 20 dB.

Compared with the classical SOMP algorithm, the procedure is similar but still has some main differences, which is summarized as follows.

- **Initial Configuration:** In the SOMP algorithm, the initial configuration of support Π is set to $\varnothing$, because no prior knowledge of the signal is available. However, in the proposed AST-SOMP algorithm, by exploiting the obtained partial channel common support in ***Step 1*** and the spatial–temporal correlation property, the initial approximation can be directly configured as the expansion of T_0, i.e., $\Pi \leftarrow T_0 \cup \{T_0 + L\} \cup \cdots \cup \{T_0 + (N_t - 1)L\}$.
- **Iteration Number:** The required number of iterations is reduced from K in SOMP to $K - \|T_0\|_0$ in AST-SOMP; hence, the computational complexity can be further reduced, making it more applicable to practical systems.
- **Sparsity Adaptive:** The channel sparsity level can be well estimated by the partial channel common support, making the algorithm adaptive to variable channel sparsity conditions.

IV. Performance Analysis

This section addresses the performance analysis of the proposed nonorthogonal time–frequency TS-based MIMO-OFDM scheme in terms of the recovery probability of the proposed AST-SOMP algorithm, the spectral efficiency, and the computational complexity.

A. Recovery Probability

To evaluate the performance of the proposed AST-SOMP algorithm compared with standard SOMP and OMP algorithms [10] as well as the SSP and BOMP algorithms [11], [12], Fig. 3 presents the correct CIR recovery probability when different lengths of nonorthogonal frequency-domain TS N_P out of $N = 4096$ subcarriers are used under the static ITU Vehicular B (ITU-VB) channel [13] with the fixed signal-to-noise ratio (SNR) of 20 dB in a 4×4 MIMO system. The correct recovery is defined as the estimation mean square error (MSE) being lower than 10^{-2}. It can be noticed from Fig. 3 that by utilizing the obtained partial channel common support and the spatial correlation, the required length of the frequency-domain TS $N_P = 75$ could guarantee the correct CIR recovery probability in AST-SOMP when $R = 1$. The number is even less than those in SSP [11] and BOMP [12] with $R = 4$ and far less than those in the standard SOMP and OMP algorithms [10]. Furthermore, we could increase the number of the measurement vectors, i.e., R, to improve the performance by

TABLE I
SPECTRAL EFFICIENCY COMPARISON[1]

OFDM Block Length	A	B	C	D	E	Proposed
2048	66.67%	44.44%	81.94%	84.76%	84.98%	85.42%
4096	80.00%	70.59%	90.44%	91.93%	92.05%	92.28%
8192	88.89%	84.85%	95.08%	95.84%	95.90%	96.02%

[1]Here A, B, C, D, and E denote the orthogonal time-domain TS based MIMO-OFDM scheme, the orthogonal frequency-domain TS based MIMO-OFDM scheme, and the orthogonal frequency-domain TS based MIMO-OFDM scheme adopting the standard OMP, the non-orthogonal frequency-domain TS based MIMO-OFDM scheme adopting the BOMP and SSP algorithms, respectively.

exploiting the temporal correlation under static or slowly varying channels. In practice, considering the tradeoff between the robustness of the CIR recovery performance and the TS overhead, we choose the length of nonorthogonal frequency-domain TSs to be $N_P = 80$ for the proposed scheme in the following simulations.

B. Spectral Efficiency

Table I compares the spectral efficiency of different schemes in a 4×4 MIMO system. For the conventional time-domain TS-based MIMO-OFDM scheme [5], the length of each time-domain TS is $M = 256$, and hence, the total TS overhead will be $N_t \times M = 1024$. For the conventional frequency-domain TS-based MIMO-OFDM scheme [6], the TS length for each transmit antenna is 256, and hence, the total TS overhead will be 1024. If the standard OMP algorithm is applied, the TS length for each transmit antenna can be reduced to 40 according to [9]. For the nonorthogonal frequency-domain TS-based schemes adopting the BOMP [12] and SSP algorithms [11], the length of TS is set to 90 and 95, respectively. Moreover, as shown in Fig. 1(b) and (c), a CP with length of 256 is also added before the OFDM block as the guard interval. In the proposed scheme, the length of the time- and frequency-domain TS is $M = 256$ and $N_P = 80$. It can be seen that the proposed time–frequency TS-based MIMO-OFDM scheme demonstrates higher spectral efficiency than its counterparts.

C. Computational Complexity

Here, we consider the computational complexity of the proposed scheme in terms of the complex multiplications step by step. 1) In ***Step 1***, the M-point circular correlation requires the complexity of $\mathcal{O}(M)$ for every received TS. 2) In ***Step 2***, the cyclicity reconstruction operation requires the complexity of $\mathcal{O}(MN_t)$ for every received frame. 3) In ***Step 3***, for each iteration, the inner product between the residual $\mathbf{R}$ and the observation matrix $\mathbf{\Phi}$ has the complexity of $\mathcal{O}(RN_P N_t L)$, and solving multiple least squares problems $\bar{\mathbf{H}}_{\Pi}^{(k)} \leftarrow (\mathbf{\Phi}_{\Pi}^H \mathbf{\Phi}_{\Pi})^{-1}\mathbf{\Phi}_{\Pi}^H \mathbf{Y}$ can be implemented with the complexity of $\mathcal{O}(RN_P(N_t K)^2)$. Thus, the total complexity of the AST-SOMP algorithm with $K - \|T_{i,0}\|_0$ iterations is $\mathcal{O}(RN_P((N_t K)^2 + N_t L)(K - \|T_{i,0}\|_0))$.

Consequently, the overall complexity is $\mathcal{O}(RM + RMN_t + RN_P((N_t K)^2 + N_t L)(K - \|T_{i,0}\|_0))$ for R successive frames.

V. SIMULATION RESULTS

This section evaluates the performance of the proposed time–frequency TS-based MIMO-OFDM scheme, of which the simulation parameters are summarized as follows: The system bandwidth is $f_S = 8$ MHz, located at the central frequency of 760 MHz; the OFDM block length and the TS length are $N = 4096$ and $M = 256$, respectively; and the six-tap ITU-VB channel model specified by the Third-Generation Partnership Project [13] is considered. The low-density parity-check-coded OFDM system adopting the well-known belief propagation algorithm with the maximum iteration number of 30 [13] is used for simulation. The modulation schemes 256-quadrature amplitude modulation (QAM) for the static channel and 16-QAM with a receiver velocity of 30 km/h are both considered.

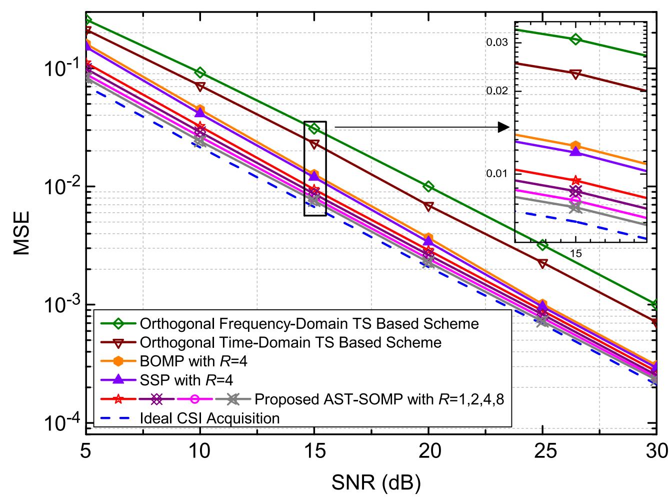

Fig. 4. Comparison of the MSE performance among different schemes under the time-varying ITU-VB channel in a 4×4 MIMO system.

Fig. 4 presents the MSE performance of different schemes under the mobile ITU-VB channel in a 4×4 MIMO system. The conventional orthogonal time- and frequency-domain TS-based schemes [5], [6], together with the nonorthogonal frequency-domain TS-based schemes adopting BOMP [12] and SSP [11] algorithms, are also evaluated for comparison. The average power of the TS or the pilot is set equal to that of the transmitted data for all the tested schemes. In addition, the MSE of the ideal CSI acquisition is illustrated as the benchmark, which shows the optimal estimation performance when the exact location of nonzero channel taps is known ***a priori***. It can be seen in Fig. 4 that the proposed AST-SOMP algorithm with $R = 1$ enjoys a significant SNR gain of 5 and 6 dB, compared with those of the conventional orthogonal time- and frequency-domain TS-based schemes, respectively, when the target MSE of 10^{-3} is considered. The SSP-based scheme could have a better performance than the BOMP-based scheme at the cost of more computational complexity. By exploiting the partial channel common support, the AST-SOMP with $R = 1$ has a slight performance improvement compared with the SSP- and BOMP-based schemes, which is in accord with Fig. 3. Furthermore, it can be seen in

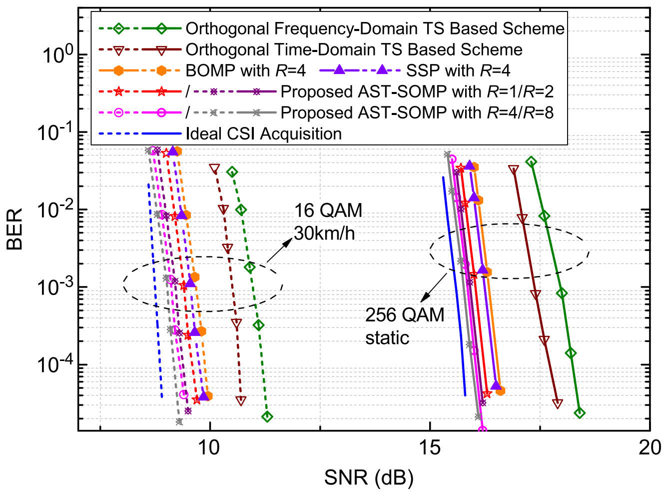

Fig. 5. BER performance comparison under the ITU-VB channel.

Fig. 4 that the performance will approach the ideal channel estimation as the number of R increases, and there still exists a gap with the ideal scenario. However, the performance improvement will not be obvious when R is larger than 4.

Fig. 5 presents the coded bit error ratio (BER) performance comparison between the proposed scheme and its counterparts in both mobile and static channels. The BER of performance with the ideal CSI acquisition is also included as the benchmark for comparison. It can be seen that the proposed scheme could support 256-QAM well under the ITU-VB channel with the BER performance close to the ideal CSI acquisition. Moreover, the proposed solution also has a better BER performance compared with other conventional schemes when lower modulation orders such as 16-QAM are adopted under the doubly selective fading channel.

VI. Conclusion Remarks

In this paper, we have proposed a spectrally efficient nonorthogonal time–frequency TS-based MIMO-OFDM scheme under the framework of SCS. The proposed scheme first utilizes the time-domain TS to obtain the partial channel common support. Then, the frequency-domain TS is used for the accurate CSI acquisition based on the proposed AST-SOMP algorithm. The AST-SOMP algorithm takes advantage of the obtained partial channel common support and the spatial–temporal correlations of the sparse MIMO channel and, hence, achieves better accuracy, more robustness, and lower complexity. Simulations have demonstrated that the proposed scheme has higher spectral efficiency and better performance than the existing schemes, which might be an appealing solution for future 5G communications.

References

[1] J. Ketonen, M. Juntti, and J. Cavallaro, "Performance-complexity comparison of receivers for a LTE MIMO-OFDM system," *IEEE Trans. Signal Process.*, vol. 58, no. 6, pp. 3360–3372, Jun. 2010.

[2] J. Geng, Z. Wei, N. Li, C. Chen, and D. Yang, "An efficient multi-user scheme for the 60 GHz wireless system with low cost arrays," in *Proc. IEEE VTC Spring*, Jun. 2013, pp. 1–5.

[3] J. G. Andrews *et al.*, "What will 5G be," *IEEE J. Sel. Areas Commun.*, vol. 32, no. 6, pp. 1065–1082, Jun. 2014.

[4] C. Jiang *et al.*, "MIMO precoding using rotating codebooks," *IEEE Trans. Veh. Technol.*, vol. 60, no. 3, pp. 1222–1227, Mar. 2011.

[5] S. K. Mohammed, A. Zaki, A. Chockalingam, and B. S. Rajan, "Highrate space–time coded large-MIMO systems: Low-complexity detection and channel estimation," *IEEE J. Sel. Topics Signal Process.*, vol. 3, no. 6, pp. 958–974, Dec. 2009.

[6] H. Minn and N. Al-Dhahir, "Optimal training signals for MIMO OFDM channel estimation," *IEEE Trans. Wireless Commun.*, vol. 5, no. 5, pp. 1158–1168, May 2006.

[7] A. L. Swindlehurst, E. Ayanoglu, P. Heydari, and F. Capolino, "Millimeter-wave massive MIMO: The next wireless revolution?" *IEEE Commun. Mag.*, vol. 52, no. 9, pp. 56–62, Sep. 2014.

[8] K. Fan and P. Tsai, "An RLS tracking and iterative detection engine for mobile MIMO-OFDM systems," *IEEE Trans. Circuits Syst. I, Reg. Papers*, vol. 62, no. 1, pp. 185–194, Jan. 2015.

[9] W. Ding, F. Yang, W. Dai, and J. Song, "Time–frequency joint sparse channel estimation for MIMO-OFDM systems," *IEEE Commun. Lett.*, vol. 19, no. 1, pp. 58–61, Jan. 2015.

[10] M. Duarte and Y. Eldar, "Structured compressed sensing: From theory to applications," *IEEE Trans. Signal Process.*, vol. 59, no. 9, pp. 4053–4085, Sep. 2011.

[11] Z. Gao, L. Dai, and Z. Wang, "Structured compressive sensing based superimposed pilot design in downlink large-scale MIMO systems," *Electron. Lett.*, vol. 50, no. 12, pp. 896–898, Jun. 2014.

[12] W. Hou and C. W. Lim, "Structured compressive channel estimation for large-scale MISO-OFDM systems," *IEEE Commun. Lett.*, vol. 18, no. 5, pp. 765–768, May 2014.

[13] L. Dai, Z. Wang, and Z. Yang, "Compressive sensing based time domain synchronous OFDM transmission for vehicular communications," *IEEE J. Sel. Areas Commun.*, vol. 31, no. 9, pp. 460–469, Sep. 2013.

[14] M. Masood, L. H. Afify, and T. Y. Al-Naffouri, "Efficient coordinated recovery of sparse channels in massive MIMO," *IEEE Trans. Signal Process.*, vol. 63, no. 1, pp. 104–118, Jan. 2015.

[15] Y. Barbotin, A. Hormati, S. Rangan, and M. Vetterli, "Estimation of sparse MIMO channels with common support," *IEEE Trans. Commun.*, vol. 60, no. 12, pp. 3705–3716, Dec. 2012.

[16] L. Boemer and M. Antweiler, "Perfect N-phase sequences and arrays," *IEEE J. Sel. Areas Commun.*, vol. 10, no. 4, pp. 782–789, May 1992.

[17] J. Candès and Y. Plan, "A probabilistic and RIPless theory of compressed sensing," *IEEE Trans. Inf. Theory*, vol. 57, no. 11, pp. 7235–7254, Nov. 2011.

[18] F. Wan, W. Zhu, and M. Swamy, "Semi-blind most significant tap detection for sparse channel estimation of OFDM systems," *IEEE Trans. Circuits Syst. I, Reg. Papers*, vol. 57, no. 3, pp. 703–713, Mar. 2010.

[19] L. Dai, Z. Wang, and Z. Yang, "Time–frequency training OFDM with high spectral efficiency and reliable performance in high speed environments," *IEEE J. Sel. Areas Commun.*, vol. 30, no. 4, pp. 695–707, May 2012.